Supporting Information

Wound microenvironment regulatory poly(L-glutamic acid) composite hydrogels containing metal-ions coordination nanoparticles for effective hemostasis and wound healing

Yanzheng Chen[1], Xueliang Zhang[1], Qing Wang[4], Chang Du[2,3]*, Chang-Ming Dong[1,]*

1. Materials

L-Glutamic acid γ-benzyl ester (BLG) was purchased from GL Biochem. 1,3-Bis(hexafluoro-α-hydroxyisopropyl) benzene (1,3-Bis-HFAB) was purchased from TCI. Triphosgene, 1-(3-dimethylaminopropyl)-3-ethylcarbodiimide hydrochloride (EDC), and N-hydroxy succinimide (NHS), dopamine (DA) hydrochloride, N, N-dimethyl ethanol amine (DMEA), hydrobromic acid (HBr, 33% in acetic acid), and trifluoroacetic acid (TFA), 3-(4,5-dimethylthiazol-2-yl)-2,5-diphenyltetrazolium bromide (MTT) and 2,2-diphenylpicrylhydrazyl (DPPH) were purchased from Adamas. The L929 mouse fibroblastic cell line, human umbilical vein endothelial cells (HUVECs), RAW264.7 was received from the Shanghai Institute of Biochemistry and Cell Biology. Streptomycin solution, reactive oxygen species assay kit (DCFH-DA fluorescence probe), Calcein/PI cell viability assay kit, 2-(4-amidinophenyl)-6-indolecarbamidine dihydrochloride (DAPI), matrix-gel™ were purchased from Beyotime. Anti-TNF-α rabbit pAb (Servicebio), anti-CD31 rabbit pAb (Servicebio), H&E Dye Set (Servicebio), Masson Dye Set (Servicebio), CD86 antibody (Affinity) and MRC1 antibody (CD206, Affinity), Alexa Fluor 488-conjugated AffiniPure goat anti-rabbit IgG (H+L) (ABclonal), EZ-press RNA Purification Kit (EZBioscience), Prime ScriptTM RT Master Mix (Takara), SYBR Green qPCR Master Mix (Bimake),

glyceraldehyde-3-phosphate dehydrogenase (GAPDH, MCE), Tegaderm (3M) and Chitosan Dressing (Qilikang) were used as received.

2. Methods and synthesis

Nuclear Magnetic Resonance Hydrogen Spectroscopy (^{1}H NMR) is measured by using the Bruker AVANCE III HD 400 spectrometer at 25 ℃. Fourier transform infrared spectroscopy (FT-IR) is performed on a Perkin Elmer Spectrum 100 at 25 ℃ and the wavelength scanning range is set at 4000-450cm^{-1}. Gel permeation chromatography (GPC) is performed on Eco-SEC HLC-8320, and DMF containing 0.01mol/L LiBr is used as the solvent, the flow rate is set at 0.6mL/min, and PMMA standard is used as the reference. Dynamic Light Scattering (DLS, Malvern ZS90) Test: uniformly disperse nanoparticles into an aqueous solution, use a nanoparticle size and Zeta potential analyzer at 25 ℃, stabilize for 60 seconds, and then perform the test. Scanning electron microscope (SEM, Phenom Pro) test: the hydrogel was frozen with liquid nitrogen, then lyophilized and sprayed by gold to observe and take photos.

2.1 Synthesis of L-glutamic acid-γ-benzyl ester N-carboxyanhydride (BLG-NCA). BLG-NCA was synthesized through the triphosgene method as previously reported.[1, 2] Briefly, BLG (2.37 g, 10 mmol) and THF (25 mL) were added sequentially under magnetic stirring, triphosgene (1.24 g, 4.2 mmol) dissolved in THF were added dropwise, and then stirred vigorously at 50 ℃ for 90 minutes. After the reaction completed, 200 mL of n-hexane was used to precipitate BLG-NCA. High-purity BLG-NCA was obtained as white needle crystals after recrystallization with a yield of 74%, and stored at -20 °C for later use.

2.2 Synthesis of poly(L-glutamic acid) benzyl ester (PBLG) and PGA. PBLG was synthesized by ring-opening polymerization of BLG-NCA in a glovebox, and the degree of polymerization was designed to be 300. Briefly, BLG-NCA (1.32 g, 5 mmol) was dissolved in 10 mL of DCM, the mixed solution of the initiator (DMEA) and catalyst (1,3-Bis-HFAB) was added into the DCM solution of BLG NCA, and then the reaction was carried out overnight. The reaction progress was monitored by using FT-

IR. The mixture was precipitated in diethyl ether, and then dried in vacuum. Finally, a white solid was obtained with a yield of 98%, and PBLG was stored at room temperature for later use.

PGA was obtained by removing the benzyl ester of PBLG. The specific steps were as follows: PBLG (500 mg, 2.31 mmol) was dissolved in TFA (10 mL) and stirred at 0 °C, followed by adding the HBr solution (2.84 mL, 11.57 mmol, 33% in acetic acid). After stirring for 2 h, the mixed solution was precipitated in diethyl ether and then washed with diethyl ether. The precipitated product was dried under vacuum, dissolved in DMSO and dialyzed in deionized water for 2 days. Finally, PGA was obtained by freeze-drying with a yield of 96% and stored at room temperature for later use.

2.3 Preparation of dopamine modified poly(L-glutamic acid) (PD) and Ox-PD PLG 129.0 mg (1 mmol) was dissolved in a mixed solvent of DMSO and DMF (DMSO: DMF = 1: 3), and 46 mg EDC·HCl (0.24 mmol) and 27.6 mg NHS (0.24 mmol) were added to activate the carboxyl group at 0 ℃ overnight. Dopamine hydrochloride 38.0 mg (0.2 mmol) and 30.0 mg (0.3 mmol) TEA were added under nitrogen atmosphere and stirred at 25 ℃ for 24 h. After the reaction, the reaction solution was dialyzed directly into 0.01 mol/L PBS buffer solution (pH 7.4). After dialysis for 24 h, deionized water was used for another dialysis for 24 h. The colorless transparent solution in the dialysis bag was collected and freeze-dried to obtain a white solid PD with a yield of 98%, which was dried and stored for later use.

The "oxidation-lyophilization" method was used as our previous method.[3] The specific steps were as follows, 0.5 wt% PD solution was oxidized by air in 0.05 M $NaHCO_3$ solution for 24 h, and then dialyzed with deionized water for 6 h to remove $NaHCO_3$. The solution was placed in a refrigerator at -18 ℃ for 24 h, and freeze-dried to obtain a gray pink foamy solid with a yield of 98 %, named Ox-PD for later use.

2.4 Preparation of metal ions coordination nanoparticles. Fe^{2+}@TA nanoparticles were prepared by using the coordination effect of $Fe^{2+}$and tannic acid (TA).[4, 5] The specific steps are as follows: 4 mL of 40 mg/mL TA solution was added with 0.1M sodium hydroxide to adjust to around 8, and then added with 8 mL of 10 mg/mL ferrous chloride solution (Fe^{2+}/TA molar ratio = 3/1). After stirring for 4 h, the nanoparticles

solution was dialyzed against a dialysis bag (MWCO = 3500) to obtain Fe^{2+}@TA nanoparticles. Note that continuous stirring is necessary to achieve a uniform and stable dispersion otherwise the nanoparticles are prone to agglomeration. Zn^{2+}@TA and Fe^{2+}-Zn^{2+}@TA nanoparticles were prepared using the same method.

2.5 Swelling performance of freeze-dried gels. For the equilibrium swelling rate test, 5 mg of spongy lyophilized hydrogel was immersed in PBS at 37 ℃ and placed in an incubator. At a predetermined time, the sample was taken from the PBS solution, gently wiped the surface moisture with filter paper, and then weighed until the weight of all samples remains unchanged (n=3). The swelling rate is calculated using the following equation: $S_R = (W_t - W_0)/W_0 \times 100\%$. S_R represents swelling rate; W_0 and W_t represent the initial weight of the lyophilized sample and the weight after the predetermined swelling time, respectively.

2.6 The photothermal conversion efficiency. The photothermal conversion efficiency (η) was calculated according to the following equation: $\eta = \frac{hA\Delta T_{max} - Q_s}{I(1 - 10^{-A\lambda})}$. Here, h is the heat transfer coefficient, A is the surface area of the container, ΔT_{max} is the maximum temperature change; Qs is the heat associated with the light absorbance, which is zero during cooling; and both I and A^{λ} are the laser power and the absorbance at 808 nm, respectively.

3. Supporting tables and figures

Table S1. The PGA composite hydrogels and physical properties.

Entry	Content		Pore size (μm)	Gelation time (s)	G' (Pa)	△T[a] (℃)	η (%)
	$P_{300}D_{20}$ (wt.%)	Metal@TA NP (wt.%)					
H	1.0	—	11.4±3.4	28±3	65.6	4.5	—
H-Zn^{2+}	1.0	0.1、Zn^{2+}@TA	15.5±5.6	29±4	268.8	5.4	—
H-Fe^{2+}	1.0	0.1、Fe^{2+}@TA	10.5±3.3	29±4	387.5	20.0	47.1
H-Fe^{2+}-Zn^{2+}	1.0	0.1、Fe^{2+}-Zn^{2+}@TA	12.6±4.0	27±4	369.1	15.7	33.4

a: this denotes that the temperature magnitude of the composite hydrogels after NIR irradiation (10 min, 808 nm, 1 W/cm^2).

Table S2 Statistical analysis of mean fluorescence intensity of immunostaining images of CD86, CD206 and CD31 in regenerated wound tissues obtained by Image J software.

Entry	CD86		CD206		CD31	
	Day 3	Day 7	Day 3	Day 7	Day 7	Day 14
PBS	75.1±2.9	46.8±1.8	2.7±0.4	6.9±0.4	15.3±0.5	11.9±1.2
Tegaderm	79.0±2.9	46.5±2.9	2.5±0.6	7.0±0.4	18.6±0.9	12.7±0.9
H	66.3±2.9	40.0±1.4	12.9±0.5	19.6±0.8	22.9±2.1	12.8±0.3
H-Fe^{2+}	70.2±1.2	39.2±2.2	2.6±0.6	15.5±0.8	18.6±0.4	13.3±0.8
H-Zn^{2+}	60.2±2.9	33.0±1.8	17.4±1.8	34.3±1.0	26.3±0.7	12.7±0.9
H-Fe^{2+}-Zn^{2+}	50.6±2.3	30.3±2.2	17.3±1.7	33.1±1.1	25.0±0.8	11.9±1.2
H-Fe^{2+}-NIR	71.3±4.2	38.6±1.8	7.9±0.7	27.1±1.2	39.1±1.3	11.1±0.7
H-Fe^{2+}-Zn^{2+}-NIR	49.5±3.5	28.6±2.2	23.6±2.2	38.7±2.1	50.4±1.8	10.9±0.5

* The values in the table represent the mean fluorescence intensity.

Table S3. qRT-PCR related primer sequences

Gene	Forward Primer Sequence	Reverse Primer Sequence
IL-1β	TTCAAGGGGACATTAGGCAG	TGTGCTGGTGCTTCATTCAT
iNOS	GCGCTCTAGTGAAGCAAAGC	AGTGAAATCCGATGTGGCCT
IL-4	GGTCTCAACCCCCAGCTAGT	GCCGATGATCTCTCTCAAGTGAT
IL-10	ACTCTTCACCTGCTCCACTG	GCTA TGCTGCCTGCTCTTAC

3.1 Synthesis and characterization of polymers

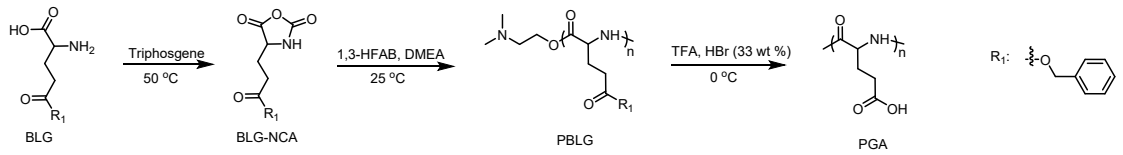

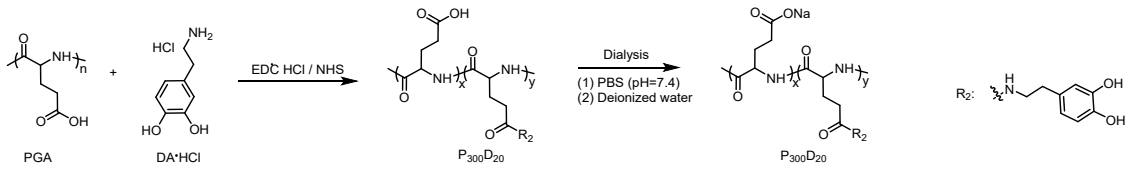

Figure S1 Synthesis of dopamine-modified PGA (PD).

The structures of the compounds and polymers during the preparation process were characterized by ^{1}H NMR. Firstly, **Figure S2A** shows the nuclear magnetic resonance and ^{1}H NMR ($CDCl_3$) of BLG NCA: δ (ppm) =7.30–7.45 (m, Ar, 5H, f), 6.62 (s, NH, 1H, b), 5.11 (s, $ArCH_2O$, 2H, e), 4.34 –4.42(t, CH, 1H, a), 2.52–2.64 (t, CH_2OCO, 2H, d), 2.02–2.34 (m, CH_2CH_2OCO, 2H, c).

The nuclear magnetic resonance (NMR) of PBLG was shown as **Figure S2B**, ^{1}H NMR ($CDCl_3$): δ = 7.23 ppm (5 H, PhCH2, h), 5.02 ppm (2 H, PhCH2O, g), 3.96 ppm (1 H, -CH2CH2CH-, d), 2.55 ppm (2 H, -CH2CH2CH-, f), 1.85-2.48 ppm (2 H, -CH2CH2CH-, e). HFAB was used as the catalyst and DMEA was used as the initiator for this reaction. Therefore, residual peaks of DMEA initiator can be observed on the NMR spectrum (δ = 2.94 ppm, -CH_2N $(CH_3)_2$, a), calculated by peak area integration, the degree of polymerization was measured to be 295, which is close to the theoretical value of 300. The GPC result in **Figure S3** indicate that the measured average molecular weight $M_{n,GPC}$ = 76.7 kDa and PDI = 1.28.

PGA was obtained by removing protective groups, dialysis, and freeze-drying. The ^{1}H NMR (D_2O) of PGA is shown in **Figure S2C**: δ = 4.35 ppm (1H, -CH_2CH_2CH-), 2.32 ppm (2H, -CH_2CH_2CH-), 1.85-2.13 ppm (2 H, -CH_2CH_2CH-). The nuclear magnetic spectrum did not show the characteristic peak of benzyl ester in **Figure S2B**, indicating that the benzyl ester protective group was removed.

$P_{300}D_{20}$ was obtained through acylation reaction, dialysis, and freeze-drying. The ^{1}H NMR (D_2O) of the nuclear magnetic resonance spectrum is shown in **Figure 2D**: δ=6.50-6.90 ppm (3H, $PhCH_2CH_2$-, a), 4.31 ppm (2H, -CH_2CH_2CH-, b), 3.35 ppm (2 H, $PhCH_2CH_2$-, c), 2.62 ppm (2 H, $PhCH_2CH_2$-, d), 2.35 ppm (2 H, -CH_2CH_2CH-, e), 1.75-2.10 ppm (2 H, -CH_2CH_2CH-, f). By integrating the a and b peaks, it can be

concluded that the grafting degree of dopamine is 20.5%, which is consistent with the theoretical value of 20.0%, indicating successful synthesis of $P_{300}D_{20}$.

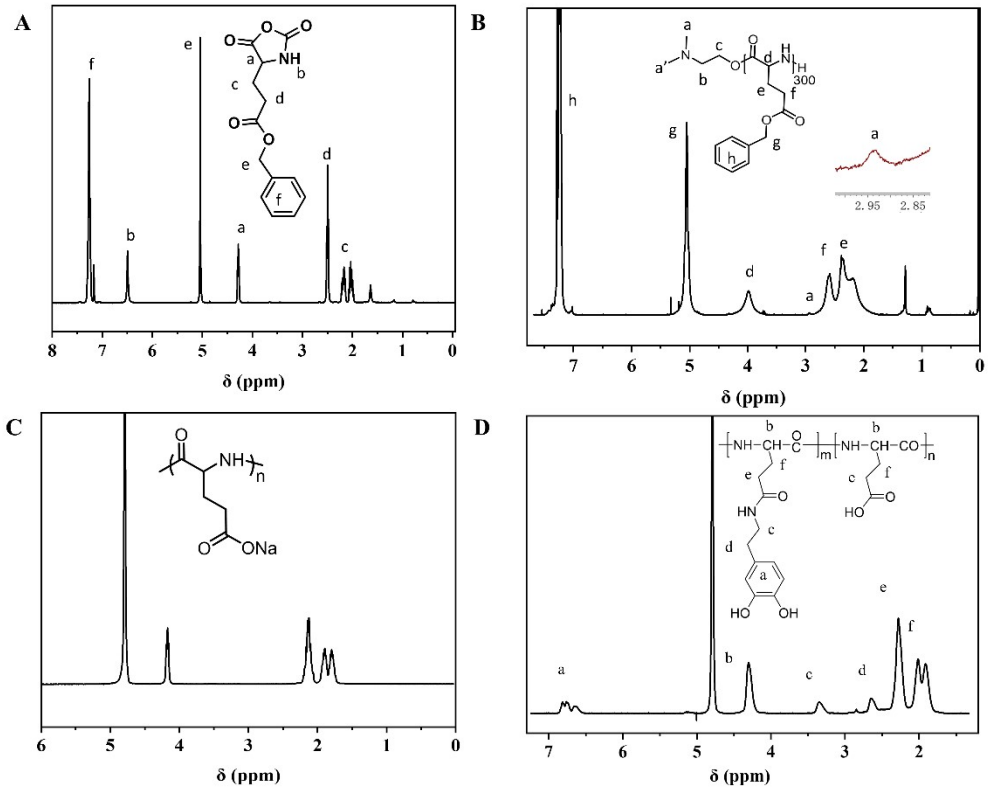

Figure S2 ^{1}H NMR spectra of (A) BLG-NCA, (B) PBLG, (C) PGA (D) $P_{300}D_{20}$.

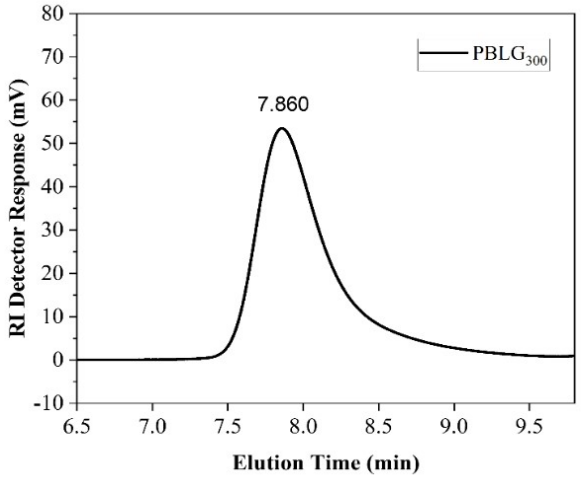

Figure S3 GPC of PBLG.

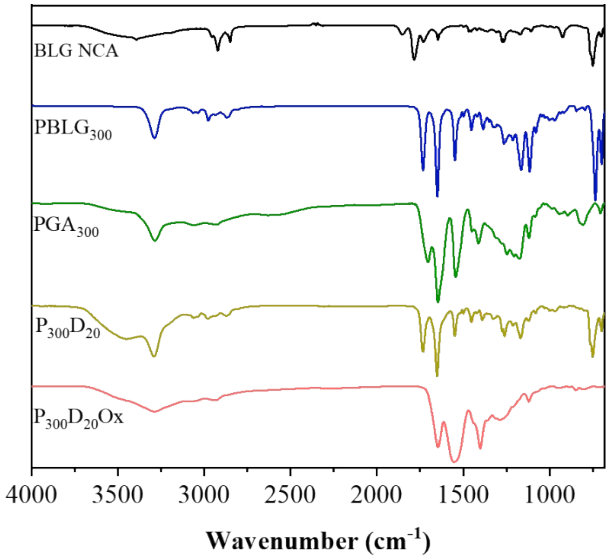

Figure S4 FT-IR of BLG NCA、PBLG、PGA、$P_{300}D_{20}$、$P_{300}D_{20}$Ox.

BLG NCA, PBLG, PGA, $P_{300}D_{20}$, and $P_{300}D_{20}$Ox were characterized by Fourier transform infrared spectroscopy. As shown in **Figure S4**, it can be seen that compared with BLG NCA, the absorption peaks of 1780 cm^{-1} and 1850 cm^{-1} belonging to the NCA ring have completely disappeared, indicating that the reaction of BLG NCA is complete and PBLG has been successfully polymerized; Then, PBLG obtained PGA by removing the benzyl protecting group, and the characteristic peak attributed to the ester group disappeared at 1734 cm^{-1} transformed to the carboxyl group at 1708 cm^{-1}; And the broad peak at 3350 cm^{-1} was assigned to the modified dopamine. So, the FT-IR data indicate successful preparation of BLG NCA, PBLG, PGA, $P_{300}D_{20}$, and $P_{300}D_{20}$Ox, which is basically with the aforementioned ^{1}H NMR.

3.2 Preparation and characterization of nanoparticles

Tannic acid (TA) has strong coordination ability with various metal ions, and we prepared 3 types of nanoparticles: Zn^{2+}@TA, Fe^{2+}@TA, and Fe^{2+}-Zn^{2+}@TA. Among them, Fe^{2+}@TA and Fe^{2+}-Zn^{2+}@TA can convert light energy into heat under infrared laser irradiation, exhibiting excellent photothermal effects, and their particle sizes were determined by DLS, as shown in **Figure S5**.

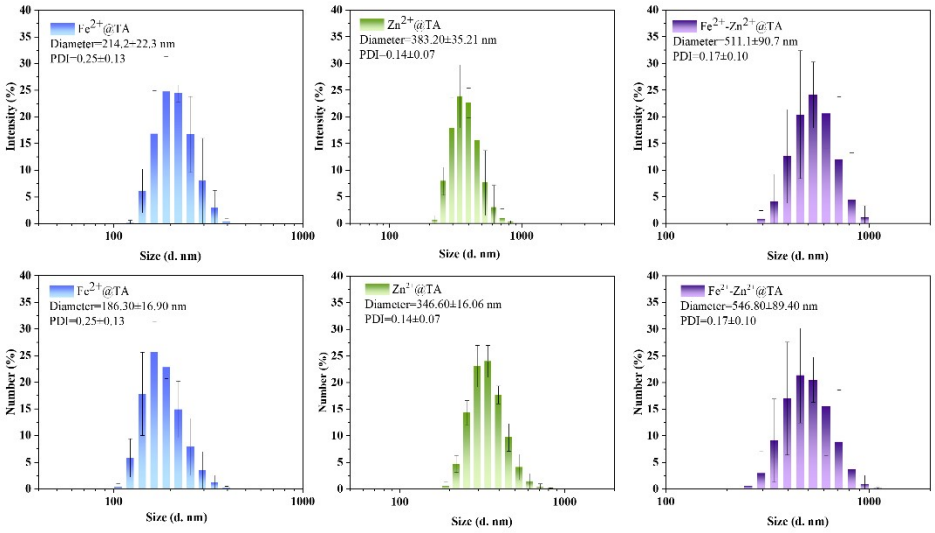

Figure S5 The DLS-determined hydrodynamic sizes of the metal ions coordinated nanoparticles including Fe^{2+}@TA, Zn^{2+}@TA and Fe^{2+}-Zn^{2+}@TA.

3.3 Characterization of hydrogels

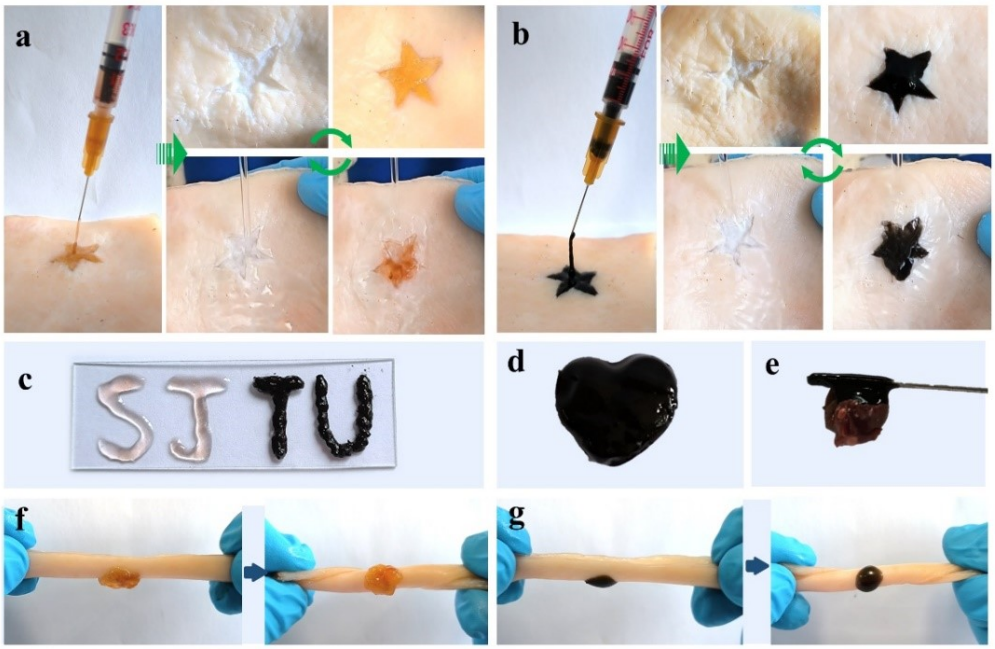

Figure S6 Injectability, molding, adhesion to rat heart, and adhesion to pig skin in a twisted state

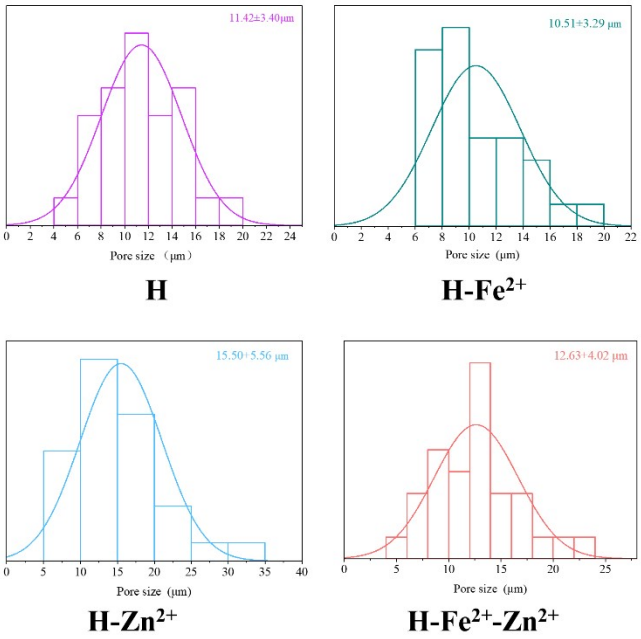

Figure S7 Pore size distribution of the freeze-dried hydrogels (n=30)

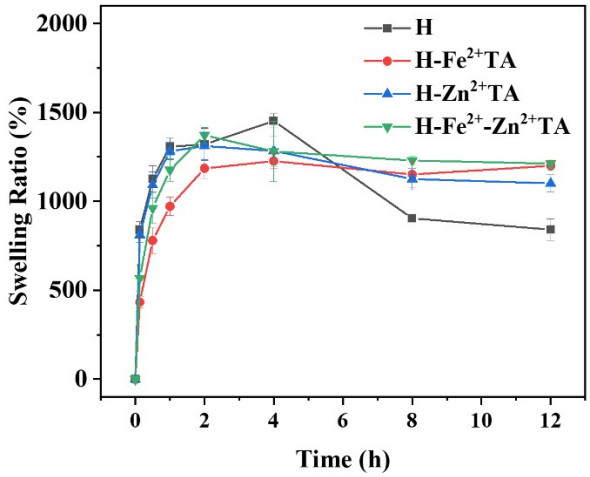

Figure S8. Swelling ratio of various freeze-dried hydrogels in 10 mM PBS at 37 ℃ (n = 3)

3.4 *In vitro* cell experiments

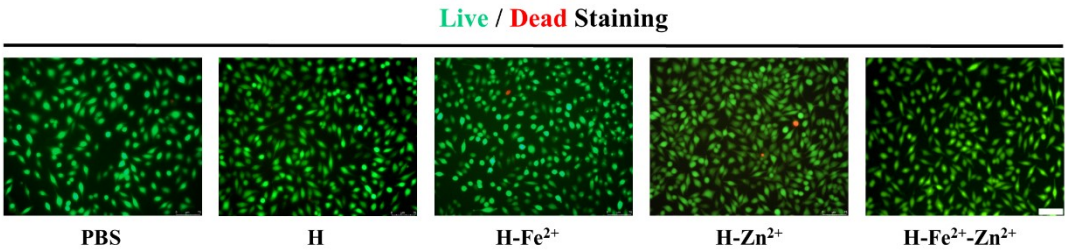

Figure S9 The representative Live/Dead cell double staining images of L929 cells when incubated on the surface of different hydrogels (scale bar = 75 μm).

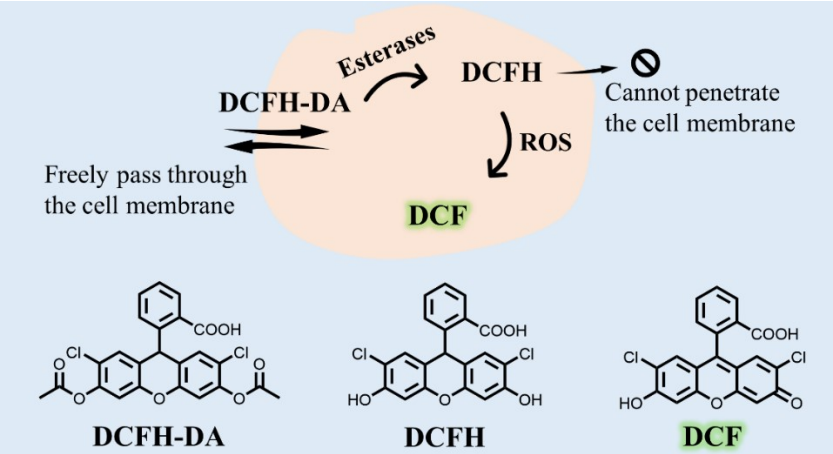

Figure S10 Schematic diagram of DCF method for detecting intracellular ROS content.

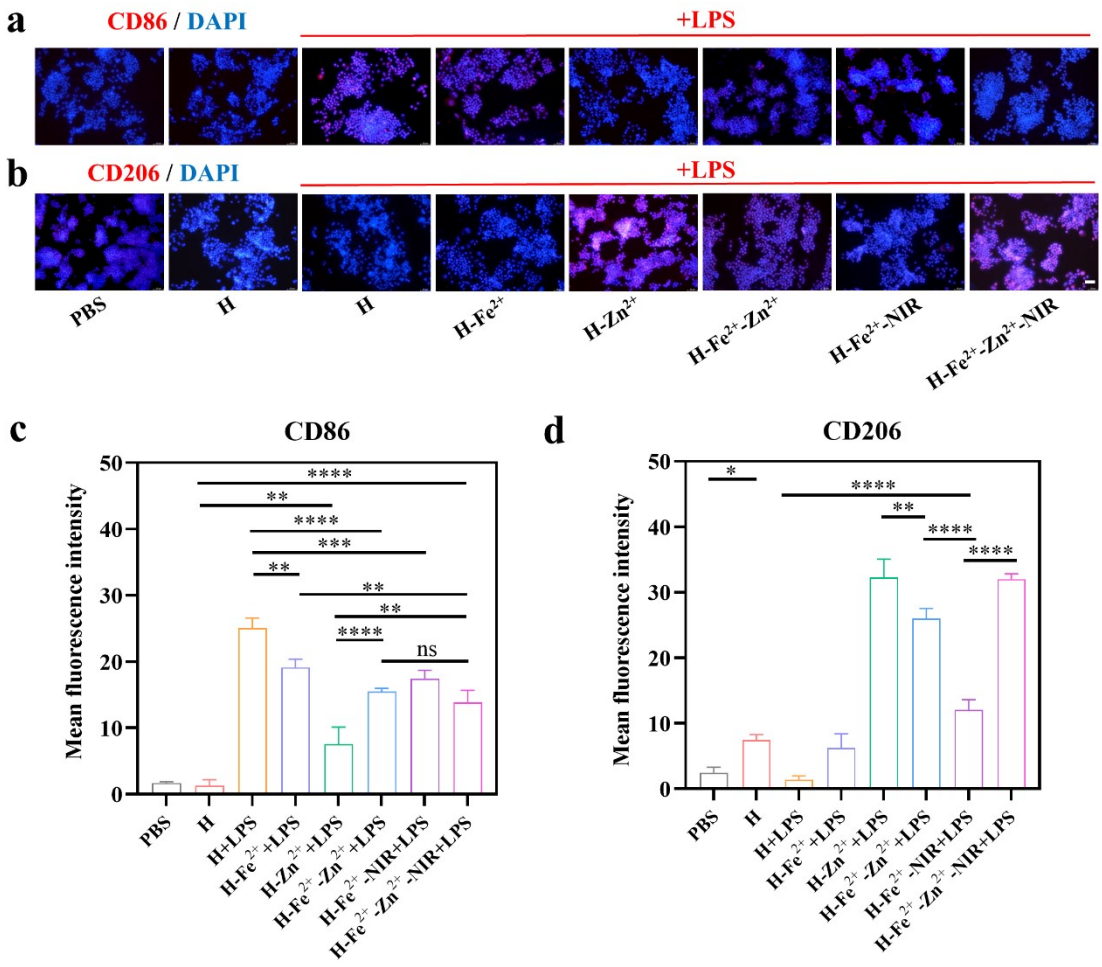

Figure S11 Immunofluorescence staining images representing (a) CD86 and (b) CD206 markers in RAW 264.7 cells (scale bar = 50 μm); Quantitative evaluation of the fluorescence area of (c) CD86 and (d) CD206 markers in RAW 264.7 cells, (n=3, * $p<0.05$, ** $p<0.01$, *** $p<0.001$, **** $p<0.0001$).

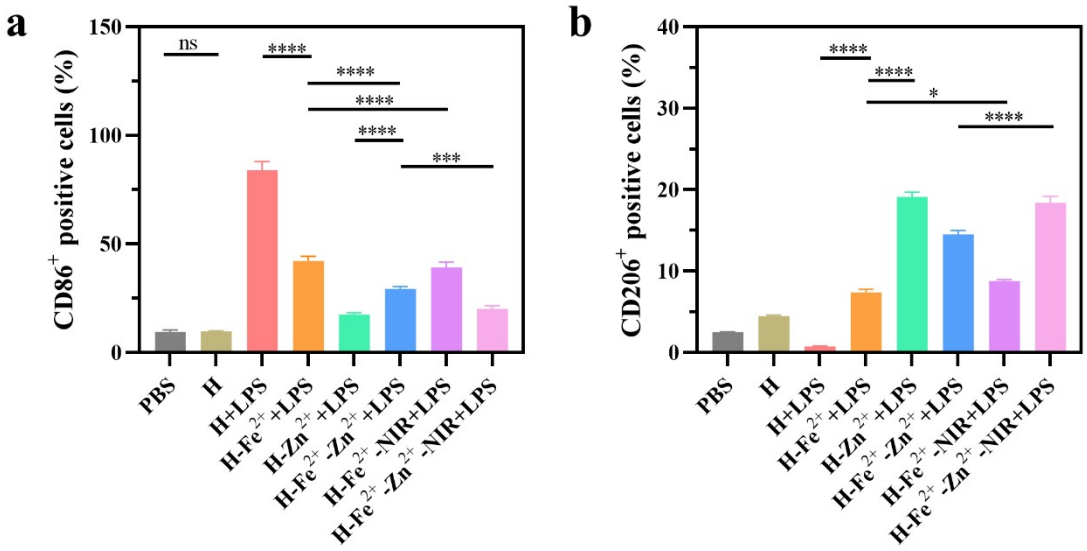

Figure S12 Statistical analysis of flow cytometry for **(a)** $CD86^+$ and **(b)** $CD206^+$ positive cells (n=3, * p<0.05, ** p<0.01, *** p<0.001, **** p<0.0001).

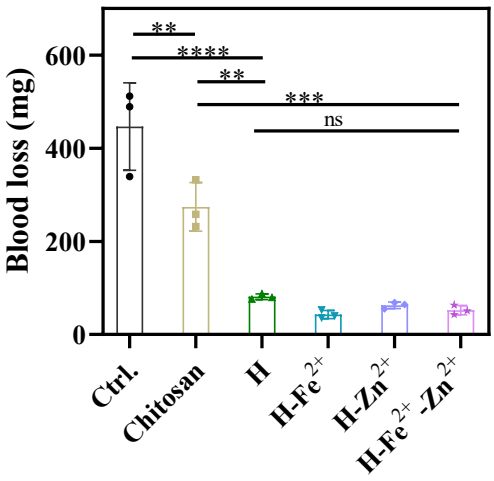

Figure S13 Blood loss of different hydrogels treated in the rat liver hemostasis.

3.5 *In vivo* healing experiments

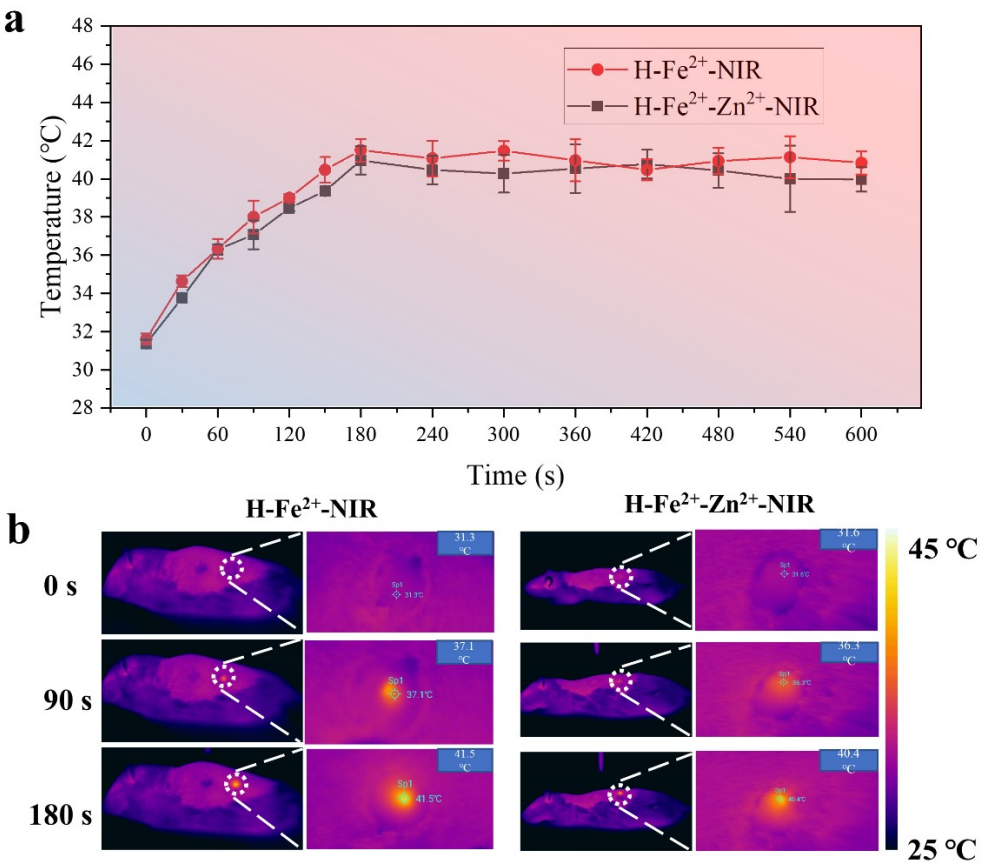

Figure S14 (a) Wound temperature curves monitored at pre-set times in SD rats; (b) Photos recorded by infrared camera in rats for the treatment groups of H-Fe^{2+}-NIR and H-Fe^{2+}-Zn^{2+}-NIR from 0 s to 90 s to 180 s, as well as local enlarged images of the wounds.

The infrared thermal image of the hydrogel in the wound area after NIR irradiation and the recorded temperature change during this process were shown in **Figure S14**. The temperature of the hydrogel on the wound rose to 40-42 °C after 3 min of NIR irradiation, which is the appropriate temperature to promote angiogenesis. By slightly adjusting the range of laser irradiation, the infrared camera was used to photograph each group of wounds, and the temperature of each wound was tracked and statistically analyzed to keep the temperature of the hydrogel at the wound at 40-42 °C.

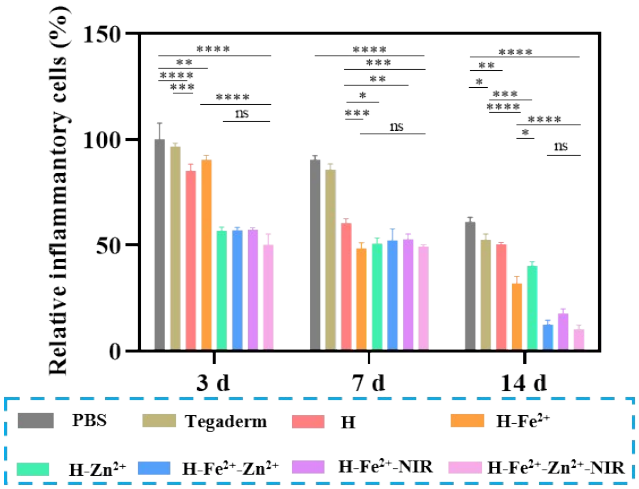

Figure S15 The relative percentage of inflammatory cells in wound regeneration tissues.

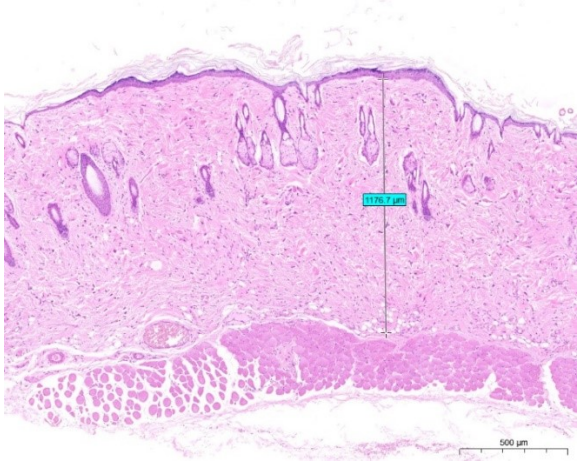

Figure S16 Representative H&E staining image of normal skin tissue of SD rat (scale bar = 500 µm).

Reference

1. S. M. Peng, Y. Chen, C. Hua and C. M. Dong, *Macromolecules*, 2009, **42**, 104-113.
2. Y. Chen, X. H. Pang and C. M. Dong, *Adv. Funct. Mater.*, 2010, **20**, 579-586.
3. Q. Bai, L. Teng, X. Zhang and C. M. Dong, *Adv Healthc Mater*, 2021, **11**, 2101809.
4. J. J. R. H. Ejima, K. Liang, J.P. Best, M.P. van Koeverden, G.K. Such, J. Cui, F. Caruso, *Science*, 2013, **34**, 154-157.
5. T. Liu, M. Zhang, W. Liu, X. Zeng, X. Song, X. Yang, X. Zhang and J. Feng, *ACS Nano*, 2018, **12**, 3917-3927.